Int. J. Heat Mass Transfer. Vol. 24, pp. 273–284
Pergamon Press Ltd. 1981. Printed in Great Britain

0017-9310/81/0201-0273 $02.00/0

FREEZING ON A FINNED TUBE FOR EITHER CONDUCTION-CONTROLLED OR NATURAL-CONVECTION-CONTROLLED HEAT TRANSFER

E. M. SPARROW, E. D. LARSON and J. W. RAMSEY
Department of Mechanical Engineering, University of Minnesota, Minneapolis, MN 55455, U.S.A.

(*Received* 30 *May* 1980 *and in revised form* 15 *July* 1980)

Abstract—Experiments were performed to study freezing on a finned vertical tube when either conduction in the solid or natural convection in the liquid controls the heat transfer. Conduction is the controlling mode when the liquid is at its fusion temperature, whereas natural convection controls when the liquid temperature is above the fusion value. The phase change medium was a paraffin, 99% pure *n*-eicosane, with a fusion temperature of 36.4°C. Auxiliary experiments were also performed with an unfinned tube to obtain comparison data. For conduction control, the enhancement of freezing due to finning is less than the area ratio of the finned and unfinned tubes, whereas for natural-convection control the enhancement is very nearly equal to the area ratio. The liquid–solid interface is a thicket of whisker-like crystals when conduction controls but is straight (i.e. vertical). On the other hand, the interface is smooth but tapered when natural convection controls—yielding bottom-heavy frozen specimens. When conduction controls, freezing continues more or less indefinitely, whereas natural convection severely retards the freezing and ultimately terminates it altogether.

NOMENCLATURE

- A, surface area;
- A_f, surface area of finned tube;
- A_{uf}, surface area of unfinned tube;
- k, thermal conductivity of solidified material;
- M, frozen mass;
- M_f, frozen mass on finned tube;
- M_{uf}, frozen mass on unfinned tube;
- T_i, temperature of cooled tube;
- ΔT_i, inner temperature difference, $T^* - T_i$;
- T_o, surface temperature of containment vessel and initial temperature of liquid;
- ΔT_o, outer temperature difference, $T_o - T^*$;
- T^*, fusion temperature;
- t, time;
- x, coordinate normal to surface.

Greek symbols

- δ, thickness of frozen layer;
- λ, latent heat of fusion;
- ρ, density of solid.

INTRODUCTION

THE NEED to find effective means of storing energy is underscored by the variability of demand and the intermittency of various of the alternative energy sources (e.g. solar). Energy may be stored in many forms, for example, electrical, thermal, potential (pumped hydro), and kinetic (flywheel). Among the thermal energy storage concepts, both sensible heat and latent heat (i.e. phase change) storage are now under investigation. The research reported here is concerned with phase-change storage.

The two thermal processes which are relevant to phase-change storage are freezing and melting. Melting occurs when energy is introduced into a solid phase-change storage medium, the actual storage being accomplished by the absorption of energy to supply the latent heat required for the conversion of solid to liquid. The extraction of energy from the medium is accomplished by the freezing of the liquid, thereby liberating the latent heat.

In the classical view of heat transfer in freezing and melting, conduction is assumed to be the sole transport mechanism and, with this assumption, the two processes are the same in all essential features. However, recent experiments have demonstrated that natural convection plays important, but different roles in freezing and in melting, thereby making the two processes highly distinct. An interesting example of this distinctiveness is encountered in the melting of a solid which is at its fusion temperature and in the freezing of a liquid which is also at the fusion point. For the former, natural convection occurs in the melt layer (subsequent to an initial transient conduction period). On the other hand, for the latter, natural convection will not occur, and the heat transfer is controlled by conduction in the frozen layer. In view of the distinctiveness of the two processes, each merits separate study. The present research is focused on the freezing process.

The aforementioned recent freezing experiments were performed with a cooled tube, either vertical or horizontal ([1] and [2] respectively), immersed in a liquid whose temperature is above the fusion temperature. Freezing takes place on the tube surface, but the rate of freezing is retarded by natural convection in the liquid. The natural convection is driven by the difference between the temperature of the freezing solid–liquid interface (i.e. the fusion temperature) and the

temperature of the bulk liquid. It was shown in [1] that natural convection can bring about complete termination of the freezing process.

The retardation of freezing and its ultimate termination are serious impediments to the heat transfer performance of phase-change thermal storage devices. Specifically, these events cause a decrease in the rate at which heat can be extracted from a storage device. It is, therefore, relevant to examine ways of enhancing heat transfer in freezing in order to redress the degradation of heat transfer performance that is inflicted by natural convection. Among potential approaches to enhancement, it is natural to consider the use of fins which extend out from the primary cooled surface into the liquid phase-change medium. Fins have served effectively to enhance other heat transfer processes (e.g. forced convection, natural convection), but it appears that their effectiveness in enhancing freezing has not been investigated.

In this paper, the heat transfer characteristics of fins used to enhance freezing will be investigated for two distinct modes of freezing. One of these is conduction-controlled freezing, whereby natural convection is absent and conduction in the solidified material is the sole heat transfer mechanism. The other is natural-convection-controlled freezing. In this mode, natural convection in the liquid severely retards and ultimately terminates the freezing.

Separate sets of experiments were carried out to study each of the aforementioned modes of freezing. All of the experiments were performed with a water-cooled, finned vertical tube immersed in a containment vessel filled with liquid *n*-eicosane, a paraffin having a melting point of 36.4°C (97.5°F). For the conduction-controlled case, the liquid paraffin was at the fusion temperature, whereas for the natural-convection-controlled case, the liquid was maintained at a temperature above the fusion value. Various freezing rates were examined by controlling the temperatures of the water-cooled tube and of the liquid paraffin.

The finned-tube data for conduction control at various freezing rates are correlated within themselves and also show remarkable agreement with a simple theory. To provide further perspectives, these finned-tube data are compared with data obtained in auxiliary experiments for an unfinned tube, also for conduction-controlled freezing. This comparison shows the enhancement that is provided by finning. The unfinned-tube data are also compared with the analytical results of [3], from which emerges an interesting conclusion about the available thermophysical properties of the paraffin [4, 5].

For the natural-convection case, two types of comparisons are made to identify the role played by the fins. One comparison involves the finned and unfinned tubes, both operated under natural convection conditions. In the other, the finned-tube results in the presence of natural convection are compared with those in which conduction was the sole transfer mechanism.

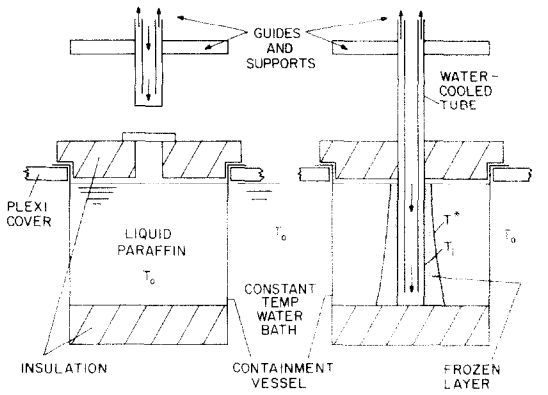

FIG. 1. Schematic diagrams of the experimental apparatus. Left-hand diagram: preparatory stage of an experiment; right-hand diagram: a data run in progress.

The results to be reported include the time variation of the frozen mass (heat extracted as a function of time), photographic information on the timewise development of the frozen layer, and layer thickness vs time data.

APPARATUS

The description of the experimental apparatus is facilitated by reference to the schematic diagrams shown in Fig. 1, which portray, respectively at the left and the right, the preparatory stage of an experiment and a data run in progress. As can be seen from these diagrams, the main components of the apparatus include a constant-temperature water bath, a stainless steel vessel for containing the phase-change medium, a water-cooled, finned copper tube on which the freezing takes place, and a system of guides and supports for positioning and holding the cooled tube. Another key component, not shown in the figure, is the system which provides and circulates temperature-controlled water through the cooled tube. Certain portions of the apparatus were adapted from that used in [1], while other parts were fabricated specifically for the present experiments.

The phase-change medium used in the experiments in *n*-eicosane paraffin, 99% pure, the freezing point of which was measured to be 36.4°C. For the experiments, the paraffin was contained in a 15.2 cm dia. cylindrical stainless steel vessel and was filled to a height of about 11.5 cm above an insulating disk which occupied the bottom of the vessel. The disk was made of 3.8 cm thick styrofoam and was coated with epoxy for strength and to avoid seepage of the paraffin into the pores of the foam.

The purpose of the aforementioned insulating disk was to avoid thermal interactions between the lower parts of the freezing specimen and the bottom wall of the containment vessel. Thermal isolation at the otherwise open top of the containment vessel was achieved with the aid of a styrofoam cap, also 3.8 cm thick. The cap was pierced by a 2.5 cm dia. hole and, in

addition, it was split into two semi-circular halves. This construction enabled the cap to be readily fitted about the water-cooled tube, subsequent to the tube's insertion into the liquid paraffin in the containment vessel.

Support of the containment vessel was accomplished with the aid of a plexiglass plate which covered the top of the constant temperature bath. As can be seen in the diagram, the vessel passed through an opening in the plate, with the lip of the vessel resting on the upper surface of the plate. To ensure its flatness over an extended period of contact with hot water, the cover plate was reinforced with angle irons. In addition to supporting the containment vessel, the plate effectively suppressed evaporation from the water surface.

The constant temperature bath consisted of a stainless steel tank, 38 cm deep and 38 × 51 cm in horizontal dimensions. The tank was well insulated at its sides and bottom and was fitted with a plexiglass cover as just described. Temperature control was accomplished by a sensing-heating-circulating unit immersed in the bath. Once a temperature level was established, it could be maintained idefinitely to better than 0.05°C. Spatial temperature uniformity throughout the bath was better than 0.1°C.

The cooled tube on which the freezing took place was made of copper, with an outside diameter of 2.506 cm and a wall thickness of 0.317 cm. Four longitudinal fins, also of copper, were installed on the outer surface of the tube. The fins were equally spaced around the circumference of the tube—90° apart. The radial length of each fin was designed to achieve a ratio of three between the surface area of the finned tube and the surface area of the unfinned tube. In actuality, the fabricated radial length was 1.92 cm, with a corresponding area ratio of 2.95.

The fins were seated in 0.159-cm deep longitudinal grooves that had been milled into the surface of the tube. Resistance-free thermal contact between the fins and the host tube was ensured by the use of silver solder. Each fin was 0.130 cm thick and 12.67 cm in axial length.

As indicated in Fig. 1, the cooled tube was, in actuality, a tube within a tube. The outer tube (i.e. the finned tube), was capped at its lower end. Cooling water entering at the top of the inner tube is conveyed to the lower end, where it turns through an angle of 180° and passes upward through the annular space between the outer and inner tubes.

Temperature measurements on the outer surface of the cooled tube were made with four thermocouples respectively positioned at the circumferential midpoints between adjacent pairs of fins. Each thermocouple was situated in a longitudinal groove machined into the surface. Once a thermocouple was installed, the groove was filled with copper oxide cement (a relatively good heat conductor), and the surface was finished so that no discontinuity between the copper oxide and the tube could be detected. The four thermocouple junctions were respectively positioned at distances of 0.635, 3.81, 6.99 and 10.16 cm from the lower end of the tube. All thermocouples were made of teflon-covered 0.0254 cm chromel and alumel wire which were calibrated specifically for these experiments.

Positioning and vertical alignment of the water-cooled tube was accomplished by a support and guide system situated above the containment vessel as indicated in the figure. In essence, this system consisted of a pair of parallel, equal-diameter, co-axial disks, each pierced by a center hole of approx. 2.54 cm in diameter. The cooled tube was passed through the center holes and, thanks to their careful alignment during the fabrication process, the tube axis was constrained to be vertical. The disks were supported by flat vertical rods anchored on the sides of the containment vessel. Radial slits were made in the disks to permit passage of the fins. In addition, each disk was fitted with a set screw which could be used to position the tube above the containment vessel.

The system which provided water to the cooled tube consisted of two units operated in series. One was a heating, refrigerating, and pumping device, in which the refrigeration portion operates continuously and temperature control is achieved by thermostatic regulation of the heating portion. This device did not provide sufficient cooling and pumping capacity for many of the investigated operating conditions. It was, therefore, supplemented by a unit consisting of a booster pump and a copper coil, both submerged in a large ice bath. The supplementary unit functioned as a pre-cooler for the heating, refrigerating, and pumping unit, so that temperature control of the water delivered to the cooled tube continued to be provided by the heater.

To enable comparisons to be made between the heat transfer characteristics for freezing on finned tubes with those for freezing on unfinned tubes, a number of data runs were made with an unfinned tube. For those runs, the water-cooled tube of [1] was employed.

EXPERIMENTAL PROCEDURE

Preparations for a data run were initiated by the addition of liquid paraffin to the containment vessel in order to replenish the paraffin removed by the freezing process of the prior run. A standard liquid fill level of approx. 11.5 cm was maintained for all of the experiments. The preparatory stage is illustrated at the left in Fig. 1. As can be seen there, the water-cooled tube is positioned above the containment vessel. Cooling water is passed through the tube during the entire preparatory period in order to ensure the attainment of temperature equilibrium between the water and the tube.

During this same period, thermal equilibrium is being established between the liquid paraffin in the containment vessel and the constant-temperature water bath. The approach of the paraffin temperature to a desired uniform value was monitored by three thermocouples immersed in the paraffin. For the runs for

natural-convection-controlled freezing, the bath temperature T_o was fixed at a value greater than the fusion temperature T^*. On the other hand, for the runs for conduction-controlled freezing, it was desired that the liquid paraffin be at the fusion temperature T^*. To attain the fusion value, the temperature of the water bath was maintained very slightly below T^*. This caused the formation of a thin frozen layer of paraffin on the inside surface of the containment vessel. After passage of a sufficient period of time, equilibrium between the frozen layer and the liquid paraffin was attained, thereby establishing temperature uniformity at the fusion value T^*.

Once both the cooled tube and the liquid paraffin had attained their respective equilibriums, the tube was immersed into the paraffin, with its lower surface resting on the insulating pad as shown in the right-hand diagram of Fig. 1. Freezing was initiated at the very instant that the tube entered the paraffin. During the entire period of the data run, both the water bath and the cooling water were maintained at their respective fixed temperatures. To terminate the data run at a preselected time, the tube was withdrawn from the liquid paraffin—passing vertically upward through the guide disks.

The removal of the frozen paraffin specimen from the cooled tube was accomplished by melting. For this purpose, the water lines to the tube were connected to the building supply, and a mixture of hot and cold water was passed through the tube. The tube wall temperature was slowly brought to the paraffin melting temperature and, at the moment of its attainment, the specimen was slipped off the tube.

Three types of data were collected from the frozen specimens. First, the frozen mass of each specimen was determined using either an analytical balance (0.1 mg accuracy) for masses up to 200 g or a double-beam balance (0.1 g accuracy) for heavier specimens. Measurements of the thickness of the frozen layer were made by mounting the specimen in a lathe and traversing the surface with a dial gage affixed to the tool post of the lathe. For this purpose, the specimen was slipped over a cylindrical mandrel which was held in the chuck of the lathe.

Photographs were taken to document the growth history of the specimens. The photographs were views of the specimen cross section, respectively at four separate cross sections starting at the top of the specimen and proceeding toward the bottom. For these cross sectional views, the specimens were sectioned by transverse cuts made on a lathe.

RESULTS AND DISCUSSION

Each data run was characterized by the values of two temperature differences and by the duration time of the run. There are three temperatures whose values influence the freezing process, namely, the temperature T_i of the cooled tube, the fusion temperature T^*, and the temperature T_o of the outer bounding surface of the liquid paraffin. The subscripts i and o respectively denote inner and outer. These temperatures affect the freezing process via the differences

$$\Delta T_i = T^* - T_i, \quad \Delta T_o = T_o - T^*. \tag{1}$$

Experiments were performed for ΔT_i values in the range from 5.6 to 27.8°C (10–50°F), whereas ΔT_o was fixed at either 0° or 17.8°C (32°F).

For the experiments involving natural convection, ΔT_i and ΔT_o (>0) were fixed and a succession of data runs, each with a progressively longer duration time, were performed. The sequence was terminated when the data indicated no further increases in the mass of the frozen specimen with increasing run time. On the other hand, for the conduction-controlled experiments, the emergence of a correlation (to be described shortly) whereby ΔT_i and the freezing time t are essentially interchangeable variables permitted a somewhat less structured selection of the parameter values.

As was noted earlier, data runs were also performed using an unfinned tube in order to facilitate comparisons with the finned-tube data.

To provide a physical perception of the appearance of a paraffin specimen that had solidified about a finned tube, reference may be made to Fig. 2. The figure is a photograph showing an angled top view of the specimen. The four lobes that radiate outward from the basic cylindrical layer are made up of paraffin which had frozen on the surfaces of the fins. Upon careful inspection, radial slits in the lobes can be detected; these slits represent the space occupied by the fins when the specimen was in place on the cooled tube. Further examination reveals that the frozen layer is tapered, increasing in thickness from top to bottom. Such a taper is characteristic of freezing controlled by natural convection, as will be demonstrated later in a more quantitative manner.

In the presentation that follows, results will first be given for conduction-controlled freezing, followed by

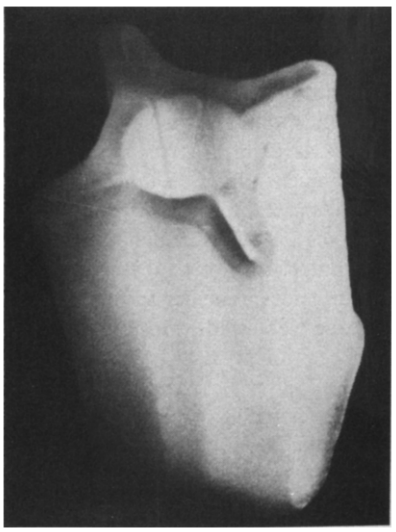

FIG. 2. Photograph of a specimen that had solidified about a finned tube.

results for natural-convection-controlled freezing. Comparisons between the two sets of results will also be made.

Conduction-controlled freezing

When freezing takes place in a liquid whose temperature is at the fusion point, the temperature distribution is uniform throughout the liquid, and natural convection will not occur. Consequently, the rate of freezing is controlled by heat conduction across the solidified layer and, in the case of a finned tube, also by heat conduction in the fins.

Conduction-controlled freezing experiments were performed for both a finned and an unfinned tube (both tubes have approximately the same outside diameter). The frozen specimens produced by these experiments are not tapered, as for the natural-convection case. Rather, their external surfaces are vertical and parallel to the axis of the cooled tube.

For both the finned and unfinned tubes, the measured values of frozen mass M corresponding to various values of the inner temperature difference ΔT_i and the freezing time t are plotted on log–log coordinates in Fig. 3. The abscissa variable is the product of $\Delta T_i t$, the motivation for which will be described shortly. Different data symbols have been used to identify the ΔT_i values to which the data correspond.

Regardless of the motivation for the use of the $\Delta T_i t$ product as the independent variable, it leads to a remarkably good correlation of the data, both for the finned and unfinned tubes. The simple model to be discussed shortly gives $M \sim (\Delta T_i t)^{1/2}$. The $\frac{1}{2}$-power provides an excellent representation of the data for the finned tube, with a corresponding least-squares equation

$$M_f = 85(\Delta T_i t)^{1/2} \tag{2}$$

with the units being those shown in Fig. 3. For the unfinned-tube data, a direct least-squares fit yields

$$M_{uf} = 29.3(\Delta T_i t)^{0.634}. \tag{3}$$

Equations (2) and (3) are dimensional and specific to the present experiments; they will shortly be related to more general representations.

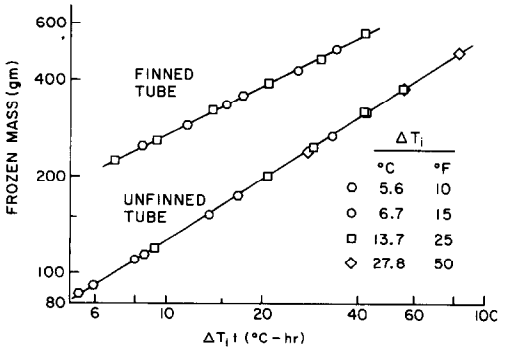

FIG. 3. Correlations of the frozen mass on finned and unfinned tubes for conduction-controlled freezing.

Figure 3 shows that the enhancement of freezing due to finning is greatest at small values of $\Delta T_i t$ (i.e. thin frozen layers) and decreases as $\Delta T_i t$ increases (i.e. as the frozen layer becomes thicker). A quantitative relationship between the two freezing configurations can be obtained by ratioing equations (2) and (3), which gives

$$M_f/M_{uf} = 2.90/(\Delta T_i t)^{0.134}. \tag{4}$$

Thus, for example, for $\Delta T_i t = 5$°C-h and 100°C-h, the corresponding values of M_f/M_{uf} are 2.34 and 1.56.

This example not only affirms that M_f/M_{uf} decreases with increasing frozen layer thickness, but also shows that

$$M_f/M_{uf} < A_f/A_{uf} \tag{5}$$

where A_f/A_{uf}, the ratio of the surface area of the finned tube to that of the unfinned tube, is 2.95. These characteristics may be rationalized by noting that the frozen layer which covers the fins acts as an insulating blanket and decreases their performance. As the freezing time increases, the thickness of the layer also increases, with a consequent reduction in fin performance. Thus, while fins are an aid to conduction-controlled freezing, it has to be recognized that the gain in frozen mass is by no means proportional to the fin surface area and that better enhancement occurs for shorter freezing times.

Attention may now be turned to generalizing the results and relating them to the literature. With a view to identifying parameters which would assist in correlating the results, the simplest case of conduction-controlled freezing was examined, namely, planar one-dimensional freezing of a liquid at its fusion temperature (Stefan problem). Furthermore, for the conditions of the present experiments, the sensible heat contribution due to subcooling of the solidified material is small compared with the latent heat contribution at the solid–liquid interface.

Then, if x represents the space coordinate measured normal to the cooled wall on which freezing occurs and $\delta(t)$ is the instantaneous thickness of the frozen layer, the governing equations for this simple model are

$$\partial^2 T/\partial x^2 = 0 \tag{6}$$

$$k\,\partial T/\partial x = \rho\lambda(\mathrm{d}\delta/\mathrm{d}t), \quad T = T^* \quad \text{at} \quad x = \delta \tag{7}$$

$$T = T_i \quad \text{at} \quad x = 0 \tag{8}$$

where λ is the latent heat and T_i represents the wall temperature (i.e. the temperature on the inner boundary of the frozen layer). From a solution of these equations, the frozen mass corresponding to a surface area A is

$$M = A(2\rho k/\lambda)^{1/2}(\Delta T_i t)^{1/2} \tag{9}$$

from which it is seen that $M \sim (\Delta T_i t)^{1/2}$.

The fact that the finned-tube frozen mass results are also proportional to $(\Delta T_i t)^{1/2}$, as shown by equation

(2), is quite remarkable. As a partial rationalization of this finding, it may be noted that for the finned tube, the cross section of the frozen solid tends toward a square with increasing freezing time; that is, the freezing front consists of four planar surfaces.

In view of the fact that the $\Delta T_i t$ dependences of equations (9) and (2) were found to be identical, it was thought not unreasonable to evaluate equation (9) for the conditions of the experiment. Thus, the area A was evaluated as A_f (the surface area of the finned tube), while k was evaluated at the overall average temperature of the solid for the experiments; values of k and λ were taken from [4] and [5], while ρ was measured during the present study. When these quantities are introduced into equation (9), there follows

$$M = 78.7(\Delta T_i t)^{1/2}. \tag{10}$$

It is remarkable that the constant coefficient of equation (10) differs by only 8% from the coefficient in equation (2) which describes the results of the finned-tube experiments. Differences of geometry and possible differences in thermal conductivity (to be discussed shortly) may be cited. Yet, despite this, equations (2) and (10) are in agreement. In view of this finding, it is tentatively suggested that equation (9) be employed as a predictive equation for finned tubes.

Conduction-controlled freezing on an unfinned tube yields a geometrically simpler frozen layer than does conduction-controlled freezing on a finned tube. Numerical finite-difference solutions for the unfinned case were performed in [3], and results deduced from those solutions will now be compared with those of experiment as already presented in Fig. 3, and in equation (3). In [3], building blocks in the form of graphs and equations are given by which M vs $\Delta T_i t$ can be determined. Graphical interpolations are required to obtain the needed information, and products of graphical and equation-deduced quantities are used in the final calculation of M. The thermophysical properties for the calculations are from [4] and [5]. The foregoing details were mentioned to indicate that the presentation in [3] gives no clue about the shape of the relationship between M and $\Delta T_i t$.

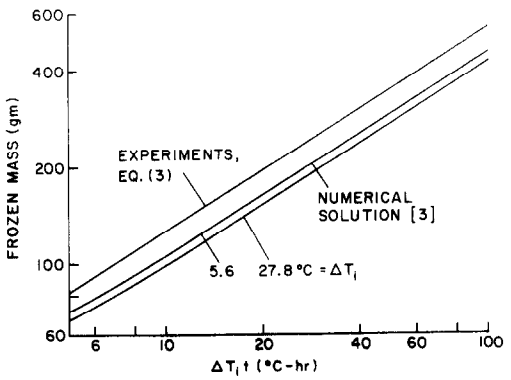

FIG. 4. Comparison of experimental and predicted frozen mass results for conduction-controlled freezing on an unfinned tube.

The comparison between the experimental results and the numerical predictions is presented in Fig. 4. From the figure, it is seen that the predictions lie about 20% below the data and that, furthermore, there is a modest separate dependence of the predictions on ΔT_i. At the larger values of $\Delta T_i t$, the prediction lines are straight (within a slight scatter attributable to graphical interpolation) and very nearly parallel to the experimental line. For smaller $\Delta T_i t$, the predictions tend to curve upward toward the experimental line.

When full consideration is given to all related factors, the agreement evidenced in Fig. 4 is surprisingly good. First of all, an error estimate [5] for the thermal conductivity data used as input to the calculations yielded $\pm 30\%$. However, of even greater significance is the fact that for conduction-controlled freezing, the experimentally encountered liquid–solid interface is not a smooth surface as is traditionally assumed in analysis. Rather, the 'surface' is a thicket of whisker-like crystals. The crystals are small for small diameter specimens (i.e. small mass M) but become quite large for larger diameter specimens. The presence of the crystals may enhance the freezing on two accounts. First, the thermal conductivity of a single crystal is normally higher than that of an amorphous material. Second, the thicket of crystals provides a much larger surface area for freezing than does a smooth interface. These considerations place the level of agreement between the experimental results and the predictions in a favorable light.

Natural-convection-controlled freezing

When the outer bounding surface of the containment vessel is maintained at a temperature T_o which exceeds the fusion temperature T^*, there is a natural convection recirculation in the liuqid. The direction of the recirculating flow is downward along the liquid–solid interface and upward along the bounding wall of the containment vessel.

The physical mechanisms by which natural convection retards and ultimately terminates freezing are discussed in detail in [1], and only a brief account need be given here. In this regard, it may be noted that the heat conducted across the solidified layer from the freezing interface to the cooled tube is the sum of two contributions: (a) the latent heat liberated by the phase change and (b) the natural convection heat transfer from the bulk liquid to the interface. As the layer grows thicker, its thermal resistance increases, with a consequent reduction in the rate of heat conduction (note that ΔT_i is constant). On the other hand, the natural convection contribution is essentially unchanging with time. Therefore, to fulfill the energy balance, the rate of freezing must decrease and ultimately go to zero.

These events are photographically documented in Fig. 5. The figure shows the cross sectional evolution of the frozen layer on the finned tube at a fixed axial station that is one-third of the way from the top to the

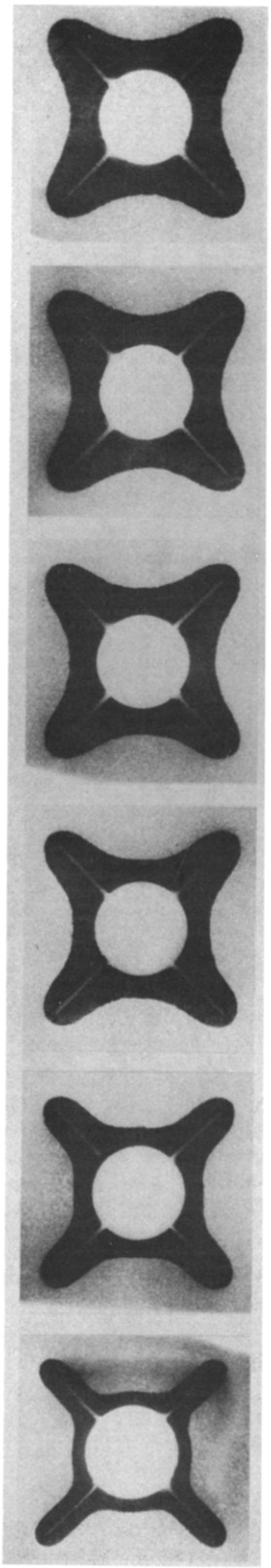

FIG. 5. Timewise evolution of the frozen layer at a fixed axial station on a finned tube for natural-convection-controlled freezing. Run times (bottom to top): 5, 15, 30, 60, 120, and 180 min; $\Delta T_i = 27.8°C$, $\Delta T_o = 17.8°C$; axial station = 1/3 of the distance from the top to the bottom of the specimen.

bottom of the frozen specimen. The successive photographs correspond respectively to run times of 5, 15, 30, 60, 120 and 180 min. and to fixed values of $\Delta T_i = 27.8°C$ and $\Delta T_o = 17.8°C$. From the figure, it can be seen that freezing is rapid at early times, but that it slows down appreciably as time passes. The cessation of freezing is clearly evident from the topmost two photographs, which show identical frozen layers.

Further perspectives about the freezing process and the development of the frozen layer can be obtained from Fig. 6. This figure contains three columns of photographs. Each column corresponds to a specific data-run duration time—5, 30, and 180 min. respectively. The four photographs in each column are cross sectional views at axial stations ranging from the top to the bottom of the specimen, with the two intermediate stations being situated 1/3 and 2/3 of the way from top to bottom. The temperature conditions are the same as those for Fig. 5 ($\Delta T_i = 27.8°C$, $\Delta T_o = 17.8°C$).

Each column of photographs enables the construction of a mental image of the shape of the frozen specimen at each selected time. At early times, the specimen is slim and the top-to-bottom taper is modest. As time advances, the freezing material tends to fill in the spaces between the fins, and this is especially true in the lower reaches of the specimen. Indeed, to an external observer, the generally square shape of the outer surface of the specimen belies the presence of the fins that are buried within the solidified material. The large-time specimens are highly tapered. The rightmost column of photographs corresponds to the final shape of the frozen layer, i.e. no further changes of shape would occur for longer run times.

By careful inspection of Figs. 5 and 6, slits in the fin lobes can be seen. These slits represent the space occupied by the fins when the specimen was in place on the finned tube. With these slits as a reference, it can be seen that there is very little growth of the frozen layer beyond the tip of the fin. Rather, the growth pattern is to fill in the space between the fins.

A more quantitative perspective on the growth pattern of the frozen layer on a finned tube is presented in Fig. 7. This figure shows the timewise evolution of the shape of the frozen layer at a circumferential location midway between the fins. This is the circumferential location most remote from the influence of the fins. The figure is made up of four panels, and in each panel the thickness of the frozen layer is plotted as a function of axial distance measured downward along the specimen.

The rightmost panel shows layer thickness profiles at six times ranging from 5 to 180 min. These profiles display the development of the tapered surface contour that is typical of natural-convection-controlled freezing. The approach of the successive profiles to the final (equilibrium) profile is also clearly evident, and it can be seen that freezing is terminated at earlier times at axial stations near the top of the specimen.

The other three panels display comparisons between

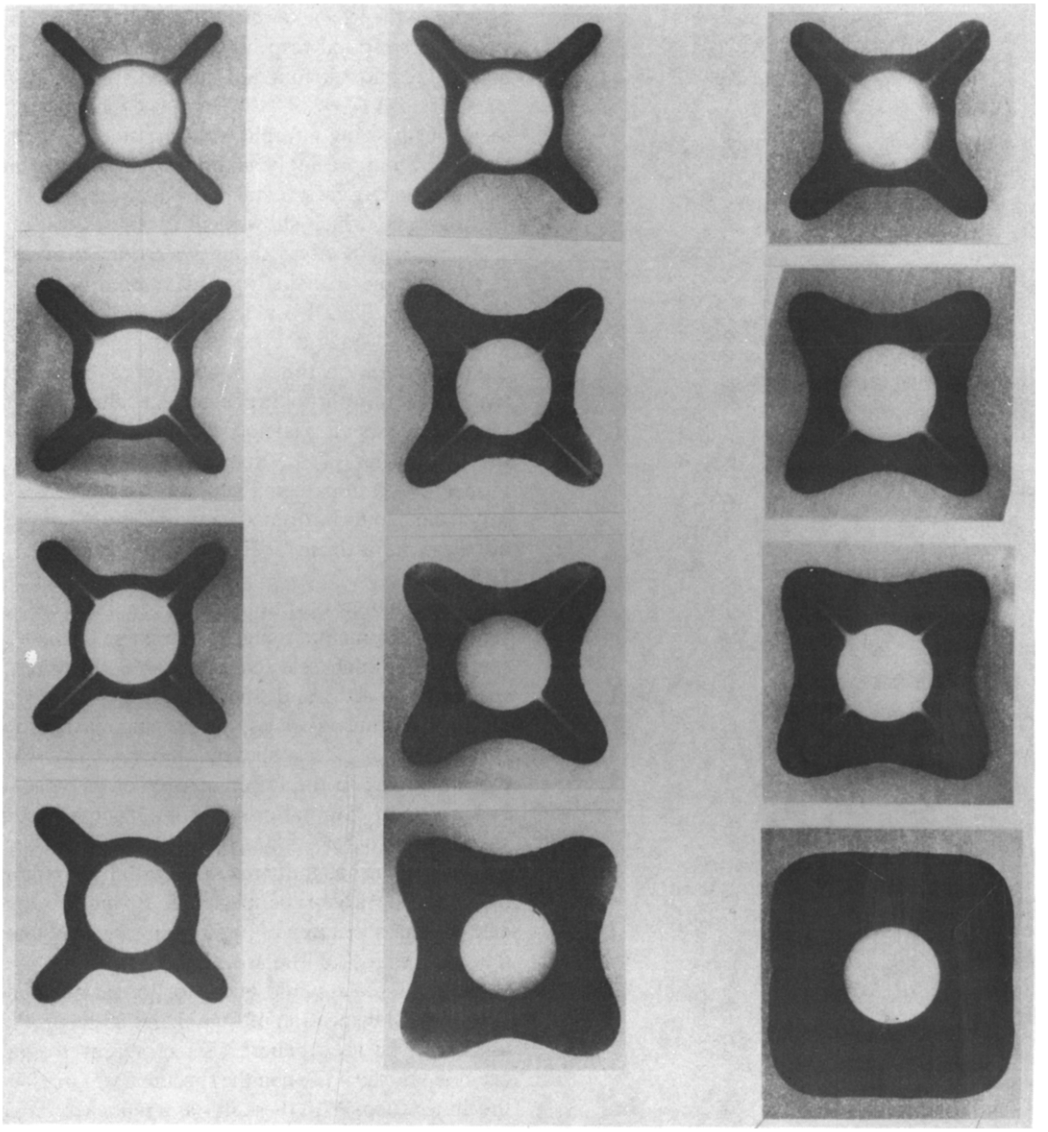

FIG. 6. Shapes of the frozen layer at various times for natural-convection-controlled freezing on a finned tube. Left column of photos: 5 min; center column: 30 min; right column: 180 min. The photos in each column correspond respectively to the top of the specimen, to axial stations 1/3 and 2/3 of the distance between top and bottom, and to the bottom. $\Delta T_i = 27.8°C$, $\Delta T_o = 17.8°C$.

the thickness profiles for finned and unfinned tubes at run times of 15, 30 and 180 min. The finned tube profiles are those midway between the fins, while those for the unfinned tubes are from [1]. It can be seen that at small times (leftmost panel), there is little difference between the frozen-layer thickness profiles for the finned and unfinned tubes. With increasing time, however, the frozen layer on the finned tube becomes substantially thicker than that on the unfinned tube.

To put this finding in perspective, it should be noted that the plotted profiles for the finned tube are at the circumferential location on the tube where the frozen layer thickness is least (i.e. midway between the fins). Thus, the use of fins not only provides additional surface area on which freezing can occur but also leads to enhanced freezing on the unfinned portion of the tube. The overall extent of the enhancement will be discussed shortly in connection with the results for the frozen mass.

The amount of energy liberated by the freezing process is closely related to the mass of the frozen material and, because of this, the mass vs time results are of practical interest. This information is conveyed in Figs. 8 and 9 for both the finned and unfinned tubes. Both of these figures correspond to an external temperature difference $\Delta T_o = 17.8°C$, with $\Delta T_i = 27.8°C$ for Fig. 8 and 13.9°C for Fig. 9.

These figures affirm the freezing pattern that is typical for natural-convection-controlled freezing. The amount of frozen mass increases sharply at small freezing times, but thereafter the rate of freezing decreases, and ultimately the freezing terminates alto-

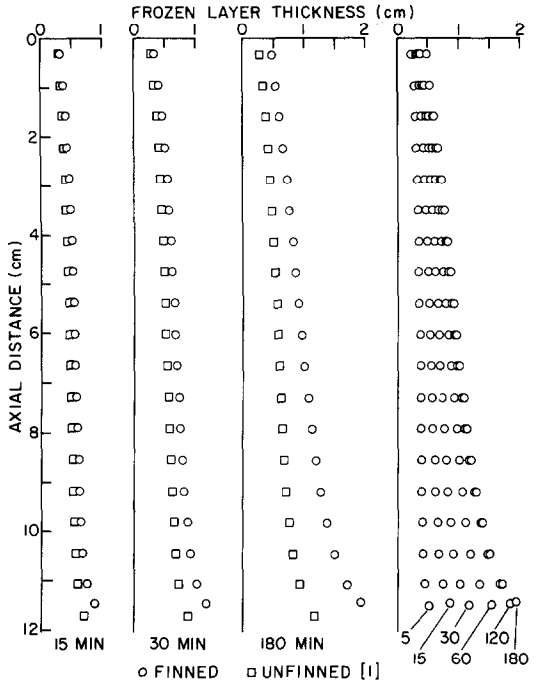

FIG. 7. Rightmost diagram: axial distributions of the frozen layer thickness at a circumferential location midway between the fins. Other diagrams: comparisons of these distributions with those for an unfinned tube [1]. $\Delta T_i = 27.8°C$, $\Delta T_o = 17.8°C$.

gether. The figures also show the significant gains that can be achieved by finning. Furthermore, the termination of freezing does not occur quite as early for the finned tube as for the unfinned tube.

It is interesting to ratio the frozen masses M_f and M_{uf} for the finned and unfinned tubes at common times. Such ratios have been determined and are listed in Table 1. The table shows a common pattern for both

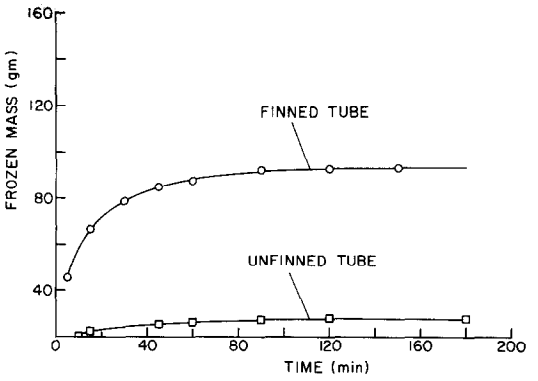

FIG. 9. Timewise variations of the frozen mass for natural-convection-controlled freezing on finned and unfinned tubes. $\Delta T_i = 13.9°C$, $\Delta T_o = 17.8°C$.

sets of operating conditions. In general, there is not a large timewise variation in the extent of the enhancement due to finning as indicated by the magnitude of M_f/M_{uf}. The smallest values of M_f/M_{uf} occur at small times, with a tendency to increase with increasing time and then to level off to a constant value.

The greater enhancements in evidence at larger times result from the aforementioned fact that the retardation and termination of freezing is not quite as rapid for a finned tube as for an unfinned tube. This somewhat extended freezing period can be rationalized by consideration of the balance between the heat conducted across the frozen layer and the additive contributions of natural convection and latent heat liberation. Owing to the presence of the fins, the conduction capabilities are enhanced, so that the balance between conduction and natural convection, which causes the eventual termination of freezing, is delayed.

It is interesting to note that the values of M_f/M_{uf}

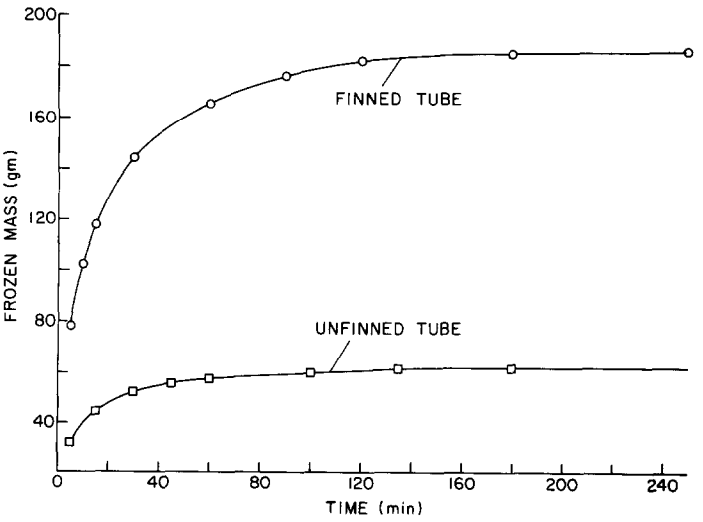

FIG. 8. Timewise variations of the frozen mass for natural-convection-controlled freezing on finned and unfinned tubes. $\Delta T_i = 27.8°C$, $\Delta T_o = 17.8°C$.

Table 1. Values of M_f/M_{uf} for natural-convection-controlled freezing

t(min)	5	15	30	45	60	90	120	180
M_f/M_{uf} (Fig. 8)	2.45	2.63	2.75	2.81	2.87	2.94	2.98	2.98
M_f/M_{uf} (Fig. 9)	2.64	2.92	3.16	3.30	3.33	3.34	3.34	

are in the range of the surface area ratio A_f/A_{uf}, which is 2.95 for these experiments. This finding should not be taken as necessarily indicating that the fin efficiency η, which is an index of the temperature uniformity of the fin, is on the order of unity. Although a rigorous calculation of η cannot be readily made for the case at hand, simple models can be formulated which suggest that η is substantially less than one. However, as was discussed in connection with Fig. 7, the presence of the fins causes enhancement of freezing on portions of the tube surface that lie between the fins. As a consequence, the total effect of the fins is to enhance the freezing as if the fin efficiency were on the order of one.

As a final comment about Figs. 8 and 9, it may be observed that there is considerably more freezing in evidence for the former than for the latter. This finding is directly related to the larger inner temperature difference ΔT_i for the former (27.8°C vs 13.9°C).

To conclude the presentation of results, the results for natural-convection-controlled freezing on a finned tube are brought together in Fig. 10 with those for conduction-controlled freezing. The figure shows results for ΔT_i values of 13.9 and 27.8°C, with $\Delta T_o = 0$ for the conduction cases and 17.8°C for the natural convection cases. For the conduction curves, equation (2) has been evaluated and plotted.

The figure forcefully shows the basic difference between the freezing patterns as they are controlled by conduction in the solid and natural convection in the liquid. When conduction controls, freezing continues indefinitely, although at a rate which diminishes somewhat with time. On the other hand, when natural convection controls, the freezing is drastically diminished and then terminates. Thus, as can be clearly seen in the figure, the degradation in heat transfer (i.e. in the frozen mass) due to the action of natural convection is heightened as time increases. It can also be verified by ratioing the corresponding curves that the degradation is greater at lower values of the inner temperature difference ΔT_i.

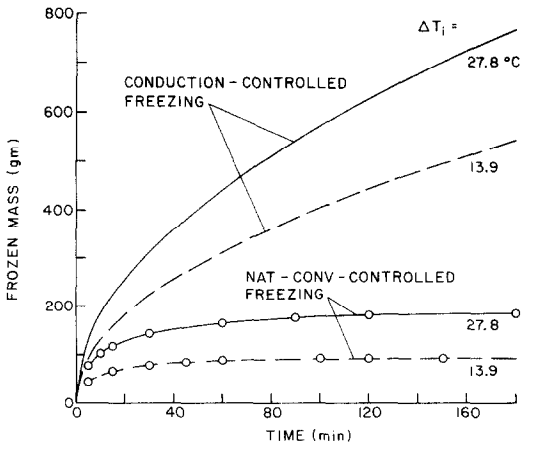

FIG. 10. Comparison of the frozen mass for conduction-controlled and natural-convection-controlled freezing on a finned tube.

CONCLUDING REMARKS

Experiments have been performed to study freezing on a finned vertical tube when either conduction in the solid or natural convection in the liquid control the heat transfer. Conduction is the controlling mode when the liquid is at the fusion temperature, whereas natural convection controls when the liquid temperature is above the fusion value. Auxiliary experiments were performed for freezing on an unfinned tube in order to provide results for comparison with those for the finned tube. A paraffin, 99% pure n-eicosane, was used in all the experiments.

The mass of the solidified material is a direct indication of the energy liberated by the freezing process. For conduction-controlled freezing, it was found that the frozen mass is very well correlated with the product $\Delta T_i t$, where ΔT_i is the temperature difference across the frozen layer and t is the freezing time. The correlation is of the form $M \sim (\Delta T_i t)^n$ where $n = 0.5$ for the finned tube and 0.634 for the unfinned tube.

For conduction-controlled freezing, the enhancement of the frozen mass due to finning is greatest when the frozen layer is thin and decreases as the layer grows thicker. The degree of enhancement is generally less than the surface area ratio of the finned and unfinned tubes.

A simple model provided results that are in remarkably good agreement with the aforementioned finned-tube correlation. For the unfinned tube, comparisons of the experimental results were made with predictions deduced from an available finite-difference solution. Deviations of about 20% were encountered, with the predictions falling low. The deviations are believed to be primarily due to the fact that for conduction-controlled freezing, the liquid–solid interface is actually a thicket of whisker-like crystals rather than a smooth surface as assumed in the analysis. Another factor of uncertainty in the predictions is the accuracy of the available thermal conductivity data of the solid.

Although the interface for conduction-controlled freezing is not smooth, it is straight (i.e. vertical). On

the other hand, when natural convection operates, the interface is smooth but there is a taper from top to bottom. At early times, the frozen specimen is slim and the taper is modest. Later, owing to the filling in of the spaces between the fins, especially near the bottom, there is a substantial taper, and the specimen is bottom heavy.

The presence of natural convection causes the freezing to be retarded and eventually to terminate altogether. The freezing terminates earlier near the top of the specimen than near the bottom. For natural-convection-controlled freezing, the enhancement of freezing due to finning is about in proportion to the additional surface area of the fins, although it is believed that the fin efficiency is substantially less than unity. The presence of the fins brings about an enhancement of freezing on the tube surface between the fins.

A comparison of results for conduction-controlled and natural-convection-controlled freezing on a finned tube shows that the degradation in heat transfer due to natural convection, is heightened as time increases. The degradation is greater at lower values of the temperature difference across the frozen layer.

Acknowledgements — This research was performed under the auspices of the U.S. Department of Energy, contract DOE/DE-AS02-79ER10343. The valuable contributions of Peter Stryker and Paulo Mendes are gratefully acknowledged.

REFERENCES

1. E. M. Sparrow, J. W. Ramsey and R. G. Kemink, Freezing controlled by natural convection, *J. Heat Transfer* **101**, 578–584 (1979).
2. A. G. Bathelt, P. D. Van Buren and R. Viskanta, Heat transfer during solidification around a cooled horizontal cylinder, in *Heat Transfer—SanDiego—*1979, *A.I.Ch.E. Symp. Ser.* **75**(189), 103–111 (1979).
3. E. M. Sparrow, S. Ramadhyani and S. V. Patankar, Effect of subcooling on cylindrical melting, *J. Heat Transfer* **100**, 395–402 (1978).
4. E. I. Griggs and W. R. Humphries, A design handbook for phase change thermal control and energy storage devices, NASA technical paper 1074 (1977).
5. E. I. Griggs and D. W. Yarbrough, Thermal conductivity of solid unbranched alkanes from *n*-hexadecane to *n*-eicosane, in *Proceedings of the 14th Southeastern Seminar on Thermal Sciences*, pp. 256–267 (1978).

CONGELATION SUR UN TUBE AILETTE AVEC UN TRANSFERT THERMIQUE CONTROLE SOIT PAR LA CONDUCTION, SOIT PAR LA CONVECTION NATURELLE

Résumé—Des expériences sur la congélation avec un tube vertical ailetté lorsque le transfert thermique est contrôlé soit par la conduction dans le solide, soit par la convection naturelle dans le liquide. La conduction est le mode qui pilote quand le liquide est à la température de fusion, tandis que la convection naturelle le fait quand la température du liquide est au dessus de la température de fusion. Le milieu considéré est une paraffine 99 pour cent de *n*-eicosane pure, avec une température de fusion de 36,4°C. Des expériences auxiliaires sont conduites aussi avec un tube lisse pour obtenir des valeurs de référence. Pour le contrôle par la conduction, l'accroissement du gel par l'ailettage est moindre que le rapport des aires des tubes avec et sans ailettes ; tandis que pour le contrôle par la convection naturelle l'accroissement est très proche du rapport des surfaces. L'interface liquide–solide est un assemblage de cristaux semblables à des whiskers quand la conduction contrôle, mais il est droit (vertical). Dans ce cas le gel continue plus ou moins indéfiniment, tandis que la convection naturelle ralentit fortement le gel et y met même fin.

ERSTARRUNGSVORGÄNGE AN EINEM RIPPENROHR BEI DURCH WÄRMELEITUNG ODER FREIE KONVEKTION BESTIMMTER WÄRMEÜBERTRAGUNG

Zusammenfassung — Es wurden Experimente durchgeführt, um den Erstarrungsvorgang an einem senkrechten Rippenrohr zu untersuchen, wobei entweder die Wärmeleitung in der festen Phase oder die freie Konvektion in der Flüssigkeit die Wärmeübertragung bestimmen. Die Wärmeleitung dominiert, wenn sich die Flüssigkeitstemperatur am Erstarrungspunkt befindet, andererseits bestimmt die freie Konvektion den Erstarrungsvorgang, wenn die Flüssigkeitstemperatur oberhalb der Schmelztemperatur liegt. Der für die Phasenumwandlung verwendete Stoff war ein Paraffin, *n*-Eicosan, mit einer Reinheit von 99% und einer Schmelztemperatur von 36,4°C. Zusätzlich wurden Experimente mit einem unberippten Rohr durchgeführt, um Vergleichswerte zu erhalten. Für den Fall, daß die Wärmeleitung dominiert, ist die Zunahme der Erstarrungsgeschwindigkeit aufgrund der Berippung geringer als das Flächenverhältnis von berippten zu unberippten Rohren, während im Falle der durch freie Konvektion beherrschten Wärmeübertragung die Zunahme ziemlich gleich dem Flächenverhältnis ist. Die Phasengrenzfläche flüssig-fest ist ein Gewirr von fadenförmigen Kristallen, wenn Wärmeleitung dominiert, sie ist aber gerade, d.h. senkrecht. Auf der anderen Seite ist die Phasengrenzfläche glatt, aber abgeschrägt, wenn natürliche Konvektion überwiegt, wobei am unteren Ende schwere Formationen ausfrieren. Wenn Wärmeleitung vorherrschend ist, dauert das Erstarren mehr oder weniger unbestimmt an, wogegen die freie Konvektion die Erstarrung stark verzögert und schließlich ganz zum Erliegen bringt.

ЗАТВЕРДЕВАНИЕ ЖИДКОСТИ НА ОРЕБРЕННОЙ ПОВЕРХНОСТИ ТРУБЫ ПРИ ПЕРЕДАЧЕ ТЕПЛА ТЕПЛОПРОВОДНОСТЬЮ ИЛИ ЕСТЕСТВЕННОЙ КОНВЕКЦИЕЙ

Аннотация — Проведены эксперименты для исследования затвердевания жидкости на оребренной поверхности вертикальной трубы при передаче тепла теплопроводностью в твердом теле или естественной конвекцией в жидкости. Теплопроводность доминирует в том случае, когда жидкость находится при температуре плавления, а естественная конвекция — когда температура жидкости выше температуры плавления. В качестве исследуемой жидкости использовался парафин (99% чистого *n*-эйкозана) с температурой плавления 36,4°С. Для сравнения были проведены также вспомогательные эксперименты на неоребренной поверхности трубы. В режиме передачи тепла теплопроводностью интенсивность затвердевания жидкости на оребренной поверхности ниже отношения площадей оребренной и неоребренной труб, в то время как в режиме естественной конвекции величина интенсивности почти равна отношению площадей. В режиме передачи тепла теплопроводностью граница раздела жидкость-твердое тело прямая (т. е. вертикальная), состоящая из множества переплетенных нитевидных кристаллов. В режиме же естественной конвекции граница раздела гладкая, но сходящаяся на конус с центром тяжести в нижней части образцов. Теплопроводность почти не оказывает влияния на процесс затвердевания, в то время как естественная конвекция существенно замедляет этот процесс и в конечном итоге полностью его останавливает.